Highlights

- Low-temperature MOCVD demonstrated the epitaxy of heavily doped n^+-Ge layers.
- Strain-relaxed P-doped Ge layer is epitaxially grown at as low as 320 °C.
- *In situ* doping realized the heavily P-doped Ge layer as high as 1×10^{20} cm^{-3}.

Epitaxial growth of heavily doped n^+-Ge layers using metal-organic chemical vapor deposition with *in situ* phosphorus doping

Shinichi Ike[1, 2], Wakana Takeuchi[1, *], Osamu Nakatsuka[1], and Shigeaki Zaima[1, 3]

[1]*Department of Crystalline Materials Science, Graduate School of Engineering, Nagoya University, Nagoya 464-8603, Japan*

[2]*Research Fellow of the Japan Society for the Promotion of Science, Tokyo 102-0083, Japan*

[3]*Institute of Materials and Systems for Sustainability, Nagoya University, Nagoya 464-8603, Japan*

Phone: +81-52-789-3819, Fax: +81-52-789-2760

*E-mail: wtakeuti@alice.xtal.nagoya-u.ac.jp

Keywords: Germanium, Phosphorus, Doping, Metal-organic chemical vapor deposition, Epitaxial growth

Abstract

We report the epitaxy of *n*-Ge layer with *in situ* phosphorus (P)-doping using metal-organic chemical vapor deposition (MOCVD) method with tertiary-butyl-germane and tri-ethyl-phosphine precursors. The crystalline and electrical properties of *n*-Ge epitaxial layers have been investigated using X-ray diffraction, atomic force microscopy, and Hall effect measurements in detail. *In situ* P-doping with MOCVD demonstrates the incorporation of P in Ge as high as 1×10^{20} cm^{-3}. The electron concentration in P-doped Ge epitaxial layers are achieved as high as 1.7×10^{19}, 1.8×10^{19}, and 2.2×10^{18} cm^{-3} at growth temperatures of 400, 350, 320 °C, respectively.

1. Introduction

Germanium (Ge) has attracted much attention as a channel material for low-power-consumption complementary metal-oxide-semiconductor (CMOS) transistors because of its higher carrier mobility than those of silicon (Si) and good compatibility with the conventional Si CMOS process. In contrast to Ge *p*MOS field-effect transistor (MOSFET), however, it is well known that the high diffusivity and the low thermal equilibrium solid solubility of *n*-type dopants (P, As, Sb) make it difficult to form high-performance n^+-Ge source/drain (S/D) junction in Ge *n*MOSFET [1].

There are some requirements for high-performance n^+-type Ge S/D structure as follows: heavily *n*-type doping with an electron concentration as high as 10^{20} cm^{-3}, formation of damage- and defect-free S/D regions including interface, and low thermal budgets to suppress the dopant diffusion out of layers. Several groups reported various doping methods for n^+-Ge to overcome the above issues [2-8]. Ion implantation method is most commonly adopted in the conventional CMOS technology, and the implantation technology requires post-implantation annealing up to 600 °C for both recrystallization and activation of the implanted-impurity in Ge. An electron concentration in Ge was achieved as high as $5–6\times10^{19}$ cm^{-3} with ion implantation method [2-4]. However, there is a concern that implantation-induced damages in the S/D regions could often degrade the electrical property of *pn* junction [5].

In this study, we focus on *in situ* doping by chemical vapor deposition (CVD) which is also a common method compatible with the conventional Si CMOS process. As reported in previous literatures [7, 8], a Ge layer with an electron concentration as high as $6–7\times10^{19}$ cm^{-3} was grown on Ge using CVD method at a low growth temperature below 400 °C, with co-flow of GeH_4 or Ge_2H_6 and PH_3 precursor gases.

We examine *in situ* phosphorus (P)-doping into Ge layers to exceed the thermal equilibrium solid solubility and to grow damage-free epitaxial layers using CVD method. P is one of preferable group-V dopant elements for Ge because of its highest solid solubility in Ge among other *n*-type dopants [1]. Additionally, as reported in the literature [8], lowering the growth temperature possibly leads to an increase of electrically active P concentration owing to the growth condition far from a thermal-equilibrium one.

Recently, it is reported that the metal-organic CVD (MOCVD) growth of undoped Ge or

$Ge_{1-x}Sn_x$ epitaxial layers at low growth temperatures of 280–350 °C [9, 10] and 320–360 °C [11, 12], respectively. Selective epitaxial growth of Ge or $Ge_{1-x}Sn_x$ on SiO_2/Si substrates at a growth temperature of 300–400 °C was also reported [13]. Thus, MO precursors have a promising potential to realize the formation of heavily doped Ge(Sn) layer selectively on S/D regions at a low temperature growth. In addition, MO precursors generally have advantages of riskless explosive, pyrophoric, and toxic compared to conventional hydride and chloride precursors for Ge epitaxy. It is expected that formation of heavily *in situ* P-doping into Ge can be realized by low-temperature MOCVD as well as the conventional *in situ* doped Ge CVD. However, there are few reports which clarify the MOCVD growth of Ge epitaxial layer with *in situ* doping. It is essentially important to comprehensively study the crystal growth of Ge layer and the crystalline properties of Ge epitaxial layers prepared by MOCVD method in order to develop heavily doped *n*-Ge S/D junctions for Ge CMOS applications.

In this study, we examined *in situ* P-doping into Ge layers epitaxially grown on Si substrate for realizing a P concentration as high as 10^{20} cm^{-3} using low-temperature MOCVD method. We also investigated the structural and electrical properties of MOCVD-grown P-doped Ge epitaxial layers.

2. Experimental procedure

All *in situ* P-doped Ge layers were grown on high-resistivity Si(001) substrates ($\rho \geq 1000$ Ω·cm). We used high-resistivity substrate in order to characterize electronic property of Ge layers with avoiding parallel conduction of the substrate. The Si substrate was chemically cleaned dipping first into an alkaline solution ($NH_4OH:H_2O_2:H_2O$=1:6:20) and second into a 1% HF solution, followed by thermal cleaning at 1000 °C for 15 min in the MOCVD chamber with a pressure of 2.4×10^3 Pa in pure H_2 ambient. Tertiary-butyl-germane (TBGe) and tri-ethyl-phosphine (TEP) were used as MO precursor gases of Ge and P, respectively, as shown in Fig. 1. H_2 and N_2 gases were simultaneously supplied into the MOCVD chamber as carrier gas. The growth temperature and growth time were 400 °C for 20 min, 350 °C for 72 min, and 320 °C for 80 min. The thicknesses of Ge layers were 245−255, 210−270, and 80 nm for the growth temperatures of 400, 350, and 320 °C, respectively. The total pressure and TBGe flow rate during MOCVD were kept at 3.0×10^3 Pa and 1.2 sccm, respectively. The TEP flow rate was ranged from 0 to 1.1 sccm. In this study, no post-deposition annealing was performed for all Ge layers.

The carrier type, carrier concentration, carrier mobility, and sheet resistance of prepared Ge layers were estimated using Hall effect measurement system with the Van der Pauw method at room temperature. The degree of strain relaxation of Ge layers were estimated using X-ray diffraction two-dimensional reciprocal space map (XRD-2DRSM; Phillips X'Pert MRD Pro diffractometer with Cu Kα1 X-ray source). XRD ω-rocking curve scan was also performed to investigate the crystalline properties of Ge layers. Scanning electron microscope (SEM; Hitachi S-5200) and atomic force microscopy (AFM; JEOL JSPM-4200) were performed to observe the surface morphology for Ge layers. Secondary ion mass spectroscopy (SIMS) was performed with a primary Cs ion beam for depth profile analysis of P atoms in Ge layers.

3. Results and discussion

Depth profiles of chemical P concentration were investigated with SIMS measurement for the P-doped Ge/Si samples grown at 400 and 350 °C with various TEP flow rates as shown in Fig. 2. These result exhibits that the chemical P concentration in the Ge layer increases with the TEP flow rate at the growth temperatures of both 400 and 350 °C. In the case of Ge growth at 400 °C, the SIMS profiles also show that the chemical P concentration gradually increases from the Ge/Si interface to the Ge surface. It is considered that this could be owing to the P segregation during the Ge growth at 400 °C. The average chemical P concentration as high as 1×10^{20} cm^{-3} is achieved for the TEP flow rate of 1.1×10^{-1} sccm, which is as high as the thermal equilibrium solid solubility of P in Ge [1].

In contrast to the conventional CVD using hydride and chloride precursors, MOCVD method often has a concern of the residual carbon (C) contamination incorporated in an epitaxial layer from MO precursors and by-product during the growth. Figures 3(a) and (b) show the SIMS depth profiles of the C concentration for the P-doped Ge/Si samples grown at 400 and 350 °C with various TEP flow rates. Moreover, Fig. 3(c) shows that the residual C concentration in the P-doped Ge layers with various growth temperatures and TEP flow rates, which were estimated from SIMS measurements. In this study, the residual C concentration were estimated from average values in the flat region of the C concentration in the Ge layers because the surface contaminants significantly influence on the C depth profiles near the Ge surface. Regardless of the growth temperature and TEP flow rate, the residual C concentration slightly increases in the ranges from 10^{17} to 10^{18} cm^{-3}, which indicates at least that increasing P incorporation up to 10^{20} cm^{-3} hardly affects residual C concentration below 10^{18} cm^{-3} in the P-doped Ge layers. In previous reports [15-17], there is an experimental evidence that the TEP gases are decomposed into ethylene (C_2H_4) and promptly exhausted as a by-product, resulting in no

C atoms or C-containing molecules left on the surface. Here, we can see peaks of the P- and C-concentration depth profile at the Ge/Si interface in Figs. 2(a), 2(b), 3(a), and 3(b). These peaks were also observed in the P-doped Ge homoepitaxial layer grown on a Ge substrate (*not shown*). These results indicate that the peak observed at the interface could be interpreted as a segregation near the interface and/or the contaminants originated from the ambient with residual MO precursors during the MOCVD process. One possibility is that the contaminants are related to pre-cleaning process of the substrate with the thermal treatment in the chamber performed in this study. There is still room to improve the surface cleaning process for reducing the contaminants on the substrate.

The crystalline property and surface morphology of P-doped Ge layers were investigated with XRD, SEM, and AFM measurements. Fig. 4(a) shows a XRD-2DRSM result obtained around the Si $\bar{2}\bar{2}4$ reciprocal lattice point for the P-doped Ge layer grown at 320 °C with a TEP flow rate of 1.1×10^{-1} sccm. The diffraction intensity of this contour map is presented on a logarithmic scale. The vertical and diagonal lines across the Si $\bar{2}\bar{2}4$ reciprocal lattice point indicate the trajectory lines of pseudomorphic and fully strain-relaxed state, respectively, for epitaxial layers. We can clearly observe two diffraction peaks related to a Si substrate and a Ge epitaxial layer, respectively, as shown in Fig. 4(a). The degree of strain relaxation (DSR) of epitaxial layer was estimated from the peak position of the Ge layer. The DSR along an in-plane direction is given by the following equation:

$$\mathrm{DSR} \equiv \frac{a_{//} - a_{\mathrm{pseud}}}{a_{\mathrm{bulk\,Ge}} - a_{\mathrm{pseud}}} \qquad (1)$$

where $a_{//}$ is the in-plane lattice constant of the Ge layer using XRD-2DRSM, $a_{\mathrm{bulk\,Ge}}$ and a_{pseud} are in-plane lattice constants of the bulk Ge and pseudomorphic Ge layer on the substrate, respectively [18]. For all P-doped Ge layers, the DSR value is estimated to be larger than 93%, which means that almost fully strain-relaxed P-doped Ge layer is grown on Si substrate.

XRD ω-rocking curves of the Ge 004 Bragg reflection were obtained to study the influence of the P incorporation on the crystallinity of P-doped Ge layers as shown in Fig. 4(b). Increasing the TEP flow rate hardly degrades the full width of half maximum (FWHM) values of Ge 004 peaks which reflect the tilting angle of Ge(004) lattice plane, for growth temperatures in the ranges of 320−400 °C. Fig. 4(b) also shows that the FWHM values increase with decreasing the growth temperature down to 320 °C. The degradation of the crystallinity of Ge epitaxial layers can be interpreted as suppressed surface migration of Ge adatoms by lowering the growth temperature.

Figs. 5 show plan-view and cross-sectional SEM images of Ge layers without and with P doping at a TEP flow rate of 1.6×10^{-2} and 1.1×10^{-1} sccm for a growth temperature of 400 °C. The SEM observations revealed that increasing in the TEP flow rate made a little change the surface morphology of Ge layers. In previous literature for heavy P-doping for Ge [8], it was reported that increasing in the chemical P concentration up to around 2×10^{20} cm^{-3} causes the degradation of the surface morphology with P agglomeration. In this study, with increasing TEP flow rate, the period of surface roughening becomes small but no significant agglomeration of P atoms on the surface was observed with SEM.

Fig. 6(a) shows AFM images of Ge layers without and with P doping at a TEP flow rate of 1.1×10^{-1} sccm for growth temperatures of 320, 350, and 400 °C, respectively. The scanning area for all images is 1×1 μm^2. Increasing the TEP flow rate little degrades the surface morphology for all samples in this study. Moreover, the root mean square (RMS) roughness of the Ge layers is drastically reduced with decreasing the growth temperature from 400 to 350 °C as shown in Fig. 6(b), which means lowering the growth temperature effectively suppresses the three-dimensional island growth of Ge layers on Si(001) substrate [19-21]. On the other hand, lowering the growth temperature down to 320 °C slightly degrades the surface morphology of the Ge layers compared with that grown at 350 °C. It is considered that reduced surface migration of Ge adatoms at low temperature might cause the surface roughening.

Considering these results of XRD and AFM measurements, heavily P-doped Ge epitaxial layer is grown on Si substrate at a growth temperature of as low as 320 °C by means of MOCVD method.

The electron concentration, carrier mobility, and sheet resistance of P-doped Ge layers were evaluated with Hall effect measurement at room temperature. For all P-doped Ge layers prepared in this study, *n*-type conduction was observed in the Hall effect measurement. Figs. 7(a) and (b) show results of the chemical P concentration, electron concentration, and sheet resistance in P-doped Ge layers as a function of the TEP flow rate for various growth temperatures. In this study, the Hall factor is assumed to be unity. As discussed above in Fig. 2(a), the SIMS measurement demonstrated the increase in the chemical P concentration in the layer with the TEP flow rate (Fig. 7(a)). The electron concentration corresponding to the electrically active P concentration were estimated to be 1.7×10^{19}, 1.8×10^{19}, 2.2×10^{18} cm^{-3} for the growth temperatures of 400, 350, 320 °C, respectively. In addition, we can also observe that the chemical P concentration drastically decreases with lowering the growth temperature even the constant TEP flow rate. At present, we consider that the decreasing the P concentration is owing to less thermal decomposition of TEP compared with that of TBGe during the low-temperature growth. The sheet resistance of P-doped Ge layers decreases with increasing in the

TEP flow rate, namely, increasing in the electron concentration as shown in Fig. 7(b). Here, we can see a plateau of electrically active P concentration of 1–2×10^{19} cm^{-3} in Fig. 7(a). It is considered that this plateau concentration is related to the thermal equilibrium solid solubility of P in Ge at the growth temperature.

Fig. 8 shows the electron concentration as a function of the chemical P concentration for P-doped Ge layers grown at different temperatures. The diagonal dashed line corresponds to the fully electrical activated P concentration in P-doped Ge layers. For P-doped Ge layers grown at 350 and 400 °C, we found that the incorporated-P atoms are almost activated up to 1–2×10^{19} cm^{-3} as donor occupying the substitutional site in Ge. In the case of the chemical P concentration as high as 1×10^{20} cm^{-3}, however, the electron concentration remained at 1.7×10^{19} cm^{-3} which corresponds to an activation ratio of 17%.

By comparison to the growth temperature of 350 and 400 °C, for that of 320 °C, the electron concentration is as low as 2.2×10^{18} cm^{-3} despite the chemical P concentration below the solid solubility of P in Ge. The activation ratio was estimated to be 23%. According to the previous report [22, 23], deactivation of *n*-type dopants in a Ge are generally interpreted as the formation of E-centers (*n*-type dopant-vacancy pair) and/or their clusters. Additionally, it is experimentally reported that the concentration of vacancy-related defects in Si/$Si_{0.64}Ge_{0.36}$/Si structures increases with decreasing the growth temperature in molecular beam epitaxy [24]. Regarding the degradation of the activation ratio at 320 °C, we considered that the incorporation of large amount of vacancies in the Ge layers owing to the low growth temperature could enhance the formation of P-vacancy pair and/or their clusters during MOCVD growth. Thus, the cluster formation possibly suppresses the activation of P atoms, resulting in the low electron concentration even though the chemical P concentration is below the solid solubility in a Ge. Considering these results, *in situ* P-doping by low-temperature MOCVD enables us to form the heavily doped *n*-Ge epitaxial layers with a concentration at least as high as the thermal equilibrium solid solubility limit of P in Ge.

Fig. 9 shows the electron concentration dependence of electron mobility for P-doped Ge layers and the bulk *n*-Ge as a reference [25]. The electron mobility for all P-doped Ge/Si samples was lower than that of the bulk *n*-Ge. The electron mobility is considered to be strongly influenced by the crystallinity of the Ge layers. The fully strain-relaxed P-doped Ge epitaxial layers prepared in this study would contain a lot of dislocations owing to the large lattice mismatch of 4.2% between Ge

and Si. As discussed in Fig. 4(b), increasing the growth temperature reduces the tilting angle of the lattice plane of epitaxial layer, in other words, improves the crystalline quality of the Ge layers. The degradation of the carrier mobility with lowering in the growth temperature can be attributed to the deterioration of the crystallinity of the Ge layers.

4. Conclusions

We investigated the crystalline and electrical properties of *in situ* P-doped Ge epitaxial layers grown on Si substrates using the MOCVD method with TBGe and TEP precursors. *In situ* P-doping by the low-temperature MOCVD demonstrated the incorporation of P in Ge epitaxial layer as high as 1×10^{20} cm^{-3}. XRD and AFM results showed that fully strain-relaxed P-doped Ge layer is epitaxially grown at as low as 320 °C. Hall effect measurements revealed that heavily *n*-Ge epitaxial layers with the electrically active P concentration of 1.7×10^{19}, 1.8×10^{19}, and 2.2×10^{18} cm^{-3} at growth temperatures of 400, 350, 320 °C, respectively, were achieved. Consequently, *in situ* P-doping with MOCVD promises the low-temperature growth of heavily *n*-Ge epitaxial layers, which are helpful for epitaxial growth technology for future Ge-based CMOS applications.

Acknowledgments

This work was partly supported by a Grant-in-Aid for Scientific Research (S) (Grant No. 26220605) from the Japan Society for the Promotion of Science (JSPS). S. I. would like to thank the support from a Grant-in-Aid for JSPS Fellows.

References

[1] J. Vanhellemont, E. Simoen, On the diffusion and activation of n-type dopants in Ge, Mater. Sci. Semicond. Process. **15** (2012) 642-655.

[2] J. Vanhellemont, E. Simoen, Brother Silicon, Sister Germanium, J. Electrochem. Soc. **154** (2007) H572-H583.

[3] C. O. Chui, L. Kulig, J. Moran, W. Tsai, K. C. Saraswat, Germanium *n*-type shallow junction activation dependences, Appl. Phys. Lett. **87** (2005) 091909.

[4] A. Satta, T. Janssens, T. Clarysse, E. Simoen, M. Meuris, A. Benedetti, I. Hoflijk, B. De Jaeger, C. Demeurisse, W. Vandervorst, P implantation doping of Ge: Diffusion, activation, and recrystallization, J. Vac. Sci. Technol. B **24** (2006) 494-498.

[5] M. Takenaka, K. Morii, M. Sugiyama, Y. Nakano, S. Takagi, Dark current reduction of Ge photodetector by GeO_2 surface passivation and gas-phase doping, Opt. Express **20** (2012) 8718-8725.

[6] W. M. Klesse, G. Scappucci, G. Capellini, J. M. Hartmann, M. Y. Simmons, Atomic layer doping of strained Ge-on-insulator thin films with high electron densities, Appl. Phys. Lett. **102** (2013) 151103.

[7] Y. Moriyama, Y. Kamimuta, Y. Kamata, K. Ikeda, A. Sakai, T. Tezuka, In situ doped epitaxial growth of highly dopant-activated n^+-Ge layers for reduction of parasitic resistance in Ge-nMISFETs, Appl. Phys. Express **7** (2014) 106501.

[8] Y. Shimura, S. A. Srinivasan, D. V. Thourhout, R. V. Deun, M. Pantouvaki, J. V. Campenhout, R. Loo, Enhanced active P doping by using high order Ge precursors leading to intense photoluminescence, Thin Solid Films **602** (2016) 56-59.

[9] Y. Inuzuka, S. Ike, T. Asano, W. Takeuchi, N. Taoka, O. Nakatsuka, S. Zaima, Epitaxial $Ge_{1-x}Sn_x$ Layers Grown by Metal-Organic Chemical Vapor Deposition Using Tertiary-butyl-germane and Tri-butyl-vinyl-tin, ECS Solid State Lett. **4** (2015) P59-P61.

[10] Y. Inuzuka, S. Ike, T. Asano, W. Takeuchi, O. Nakatsuka, S. Zaima, Characterization of crystallinity of $Ge_{1-x}Sn_x$ epitaxial layers grown using metal-organic chemical vapor deposition, Thin Solid Films **602** (2016) 7-12.

[11] K. Suda, S. Ishihara, N. Sawamoto, H. Machida, M. Ishikawa, H. Sudoh, Y. Ohshita, A. Ogura, $Ge_{1-x}Sn_x$ Epitaxial Growth on Ge Substrate by MOCVD, ECS Trans. **64** (2014) 697-701.

[12] K. Suda, T. Kijima, S. Ishihara, N. Sawamoto, H. Machida, M. Ishikawa, H. Sudoh, Y. Ohshita, A. Ogura, Growth of Ge Homoepitaxial Films by Metal-Organic Chemical Vapor Deposition Using t-$C_4H_9GeH_3$, ECS J. Solid State Sci. Technol. **4** (2015) P152-P154.

[13] T. Washizu, S. Ike, Y. Inuzuka, W. Takeuchi, O. Nakatsuka, S. Zaima, Selective epitaxial growth of $Ge_{1-x}Sn_x$ on Si by using metal-organic chemical vapor deposition, J. Cryst. Growth **468** (2017) 614-619.

[14] R. G. Wilson, F. A. Stevie, C. W. Magee, Secondary Ion Mass Spectrometry: A Practical Handbook for Depth Profiling and Bulk Impurity Analysis, John Wiley & Sons, New York, 1989.

[15] G. Kaneda, N. Sanada, Y. Fukuda, HREELS study of triethylphosphine (TEP) and tertiarybutylphosphine (TBP) on a Si(001)-(2×1) surface, Surf. Sci. **377** (1997) 724-727.

[16] G. Kaneda, J. Murata, T. Takeuchi, Y. Suzuki, N. Sanada, Y. Fukuda, Adsorption and decomposition of triethylphosphine (TEP) and tertiarybutylphosphine (TBP) on Si(001) studied by XPS, HREELS, and TPD, Appl. Surf. Sci. **113-114** (1997) 546-550.

[17] Y.-H. Lai, C.-T. Yeh, Hong-Ji Lin, Chien-Te Chen, W.-H. Hung, Adsorption and decomposition of triethylphosphine (TEP) and tertiarybutylphosphine (TBP) on Si(001) studied by XPS, HREELS, and TPD, J. Phys. Chem. B **106** (2002) 1722-1727.

[18] Y. Shimura, S. Takeuchi, O. Nakatsuka, B. Vincent, F. Gencarelli, T. Clarysse, W. Vandervorst, M. Caymax, R. Loo, A. Jensen, D. Petersen, S. Zaima, In-situ Ga doping of fully strained $Ge_{1-x}Sn_x$ heteroepitaxial layers grown on Ge(001) substrates, Thin Solid Films **520** (2012) 3206-3210.

[19] M. Asai, H. Ueba, C. Tatsuyama, Heteroepitaxial growth of Ge films on the Si(100)-2×1 surface, J. Appl. Phys. **58** (1985) 2577-2583.

[20] A. Sakai, T. Tatsumi, Ge growth on Si using atomic hydrogen as a surfactant, Appl. Phys. Lett. **64** (1994) 52-54.

[21] J. Knall, J. B. Pethica, Growth of Ge on Si(100) and Si(113) studied by STM, Surf. Sci. **265** (1992) 156-167.

[22] V. P. Markevich, I. D. Hawkins, A. R. Peaker, K. V. Emtsev, V. V. Emtsev, V. V. Litvinov, L. I. Murin, L. Dobaczewski, Vacancy-group-V-impurity atom pairs in Ge crystals doped with P, As, Sb, and Bi, Phys. Rev. B **70** (2004) 235213.

[23] A. Chroneos, Dopant-vacancy cluster formation in germanium, J. Appl. Phys. **107** (2010) 076102.

[24] A. P. Knights, R. M. Gwilliam, B. J. Sealy, T. J. Grasby, C. P. Parry, D. J. F. Fulgoni, P. J. Phillips, T. E. Whall, E. H. C. Parker, P. G. Coleman, Growth temperature dependence for the formation of vacancy clusters in $Si/Si_{0.64}Ge_{0.36}/Si$ structures, J. Appl. Phys. **89** (2001) 76-79.

[25] V. I. Fistul, M. I. Iglitsyn, E. M. Omelyanovskii, Mobility of Electrons in Germanium Strongly Doped with Arsenic, Sov. Phys. Solid State **4** (1962) 784.

Figure Captions

Figure 1: Chemical structural formulas of (a) tertiary-butyl-germane and (b) tri-ethyl-phosphine used as the Ge and Sn precursors, respectively.

Figure 2: SIMS depth profiles of chemical P concentration for the P-doped Ge/Si samples grown at (a) 400 and (b) 350 °C with various TEP flow rates.

Figure 3: SIMS depth profiles of C concentration for the P-doped Ge/Si samples grown at (a) 400 and (b) 350 °C with various TEP flow rates. (c) Residual C concentration in the P-doped Ge layers with various growth temperatures and TEP flow rates.

Figure 4: (a) XRD-2DRSM result of the P-doped Ge/Si sample grown at 320 °C with a TEP flow of 1.1×10^{-1} sccm and (b) FWHM values of the Ge 004 peaks of undoped- and P-doped Ge/Si samples as a function of the TEP flow rate. The thicknesses of Ge layers were 245−255, 210−270, and 80 nm for the growth temperatures of 400, 350, and 320 °C, respectively.

Figure 5: (a)−(c) Plan-view and (d)−(f) cross-sectional SEM images of Ge layers without and with P doping at TEP flow rate of 1.6×10^{-2} and 1.1×10^{-1} sccm for growth temperature of 400 °C.

Figure 6: (a) 1×1 μm^2 AFM images of Ge and P-doped Ge layers grown at 400, 350, and 320 °C with a TEP flow of 1.1×10^{-1} sccm. (b) RMS roughness of the Ge layers as a function of the TEP flow rate. The thicknesses of Ge layers were 245−255, 210−270, and 80 nm for the growth temperatures of 400, 350, and 320 °C, respectively.

Figure 7: The TEP flow rate dependence of (a) the electron concentration, the chemical P concentration (from SIMS), and (b) The TEP flow rate dependence of the sheet resistance in P-doped Ge layers. The Hall factor is assumed to be unity. The thicknesses of Ge layers were 245−255, 210−270, and 80 nm for the growth temperatures of 400, 350, and 320 °C, respectively.

Figure 8: Electron concentration as a function of chemical P concentration for P-doped Ge layers grown at difference temperatures. The dashed line corresponds to fully electrical activated P concentration.

344 **Figure 9:** Electron concentration dependence of electron mobility for P-doped Ge layers for
345 difference growth temperatures.

Fig. 1

(a) Tertiary-butyl-germane

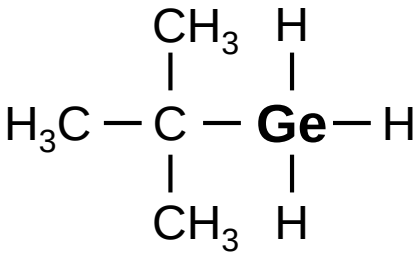

(b) Tri-ethyl-phosphine

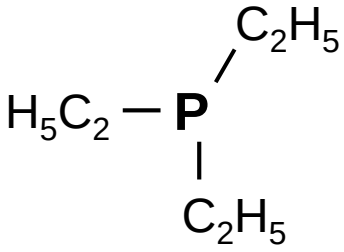

Fig. 2

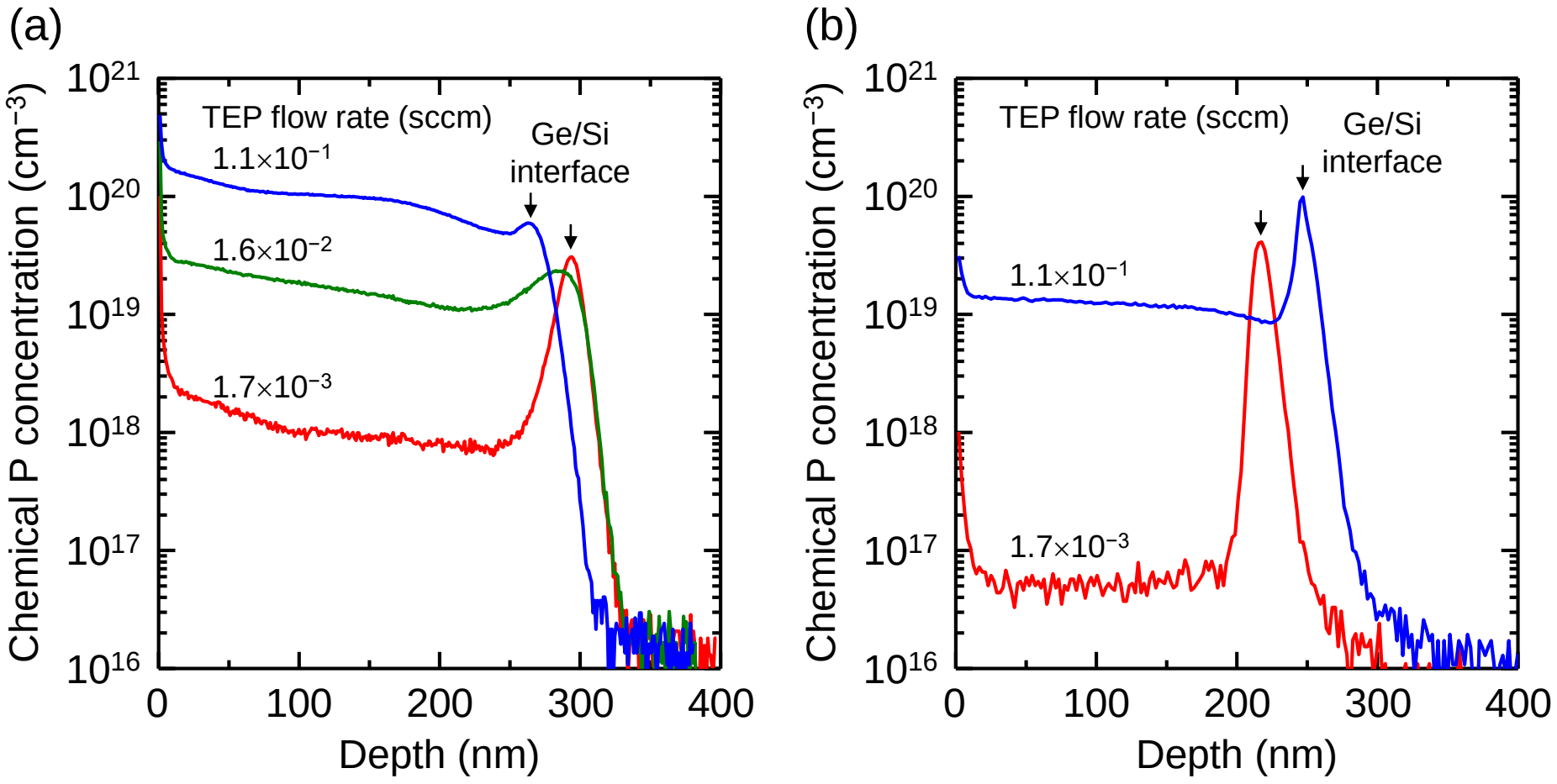
(a)
(b)
Chemical P concentration (cm^{-3})
10^{21}
10^{20}
10^{19}
10^{18}
10^{17}
10^{16}
TEP flow rate (sccm)
1.1×10^{-1}
1.6×10^{-2}
1.7×10^{-3}
Ge/Si interface
0
100
200
300
400
Depth (nm)

Fig. 3

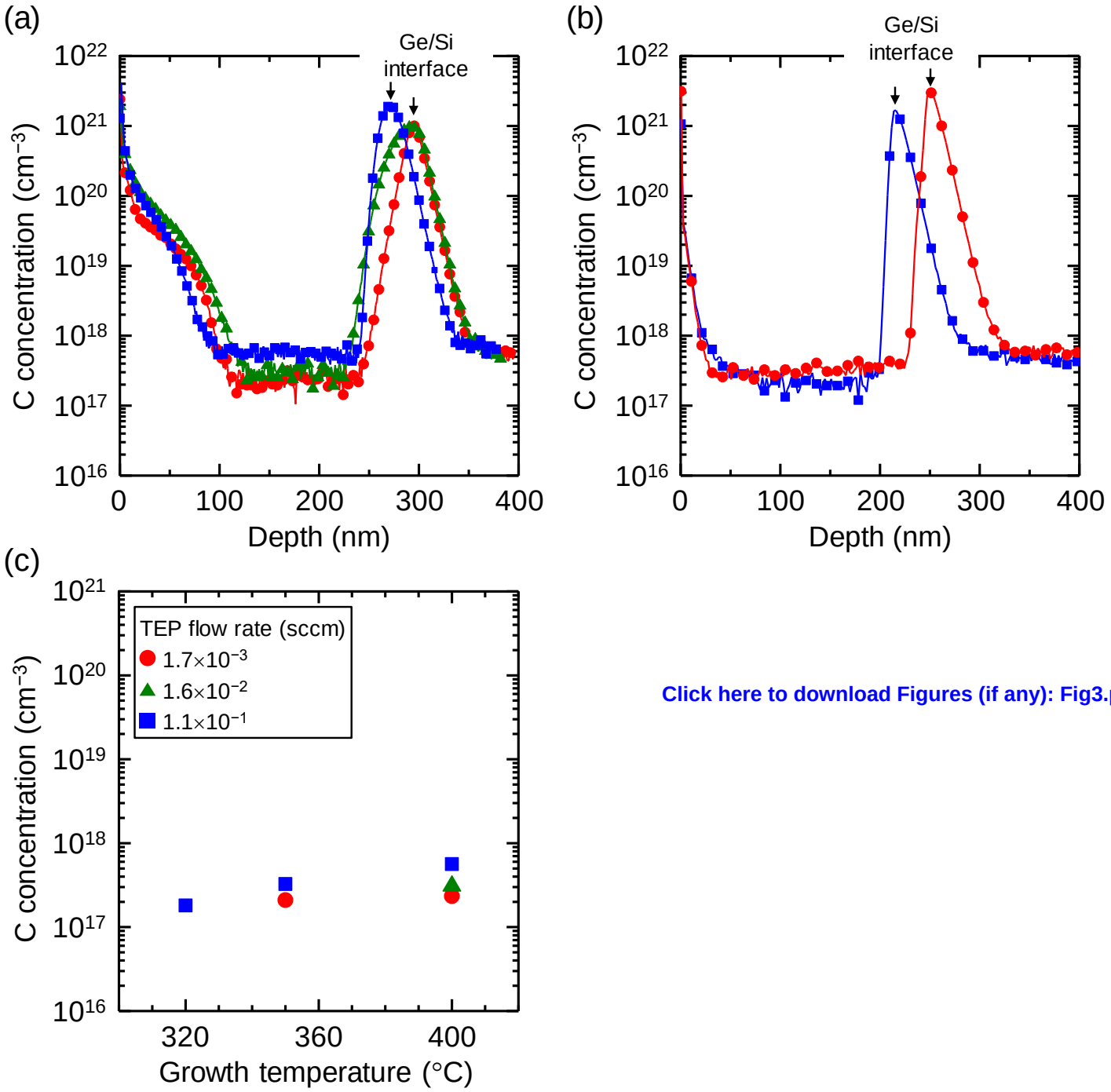

Click here to download Figures (if any): Fig3.pdf

Fig. 4

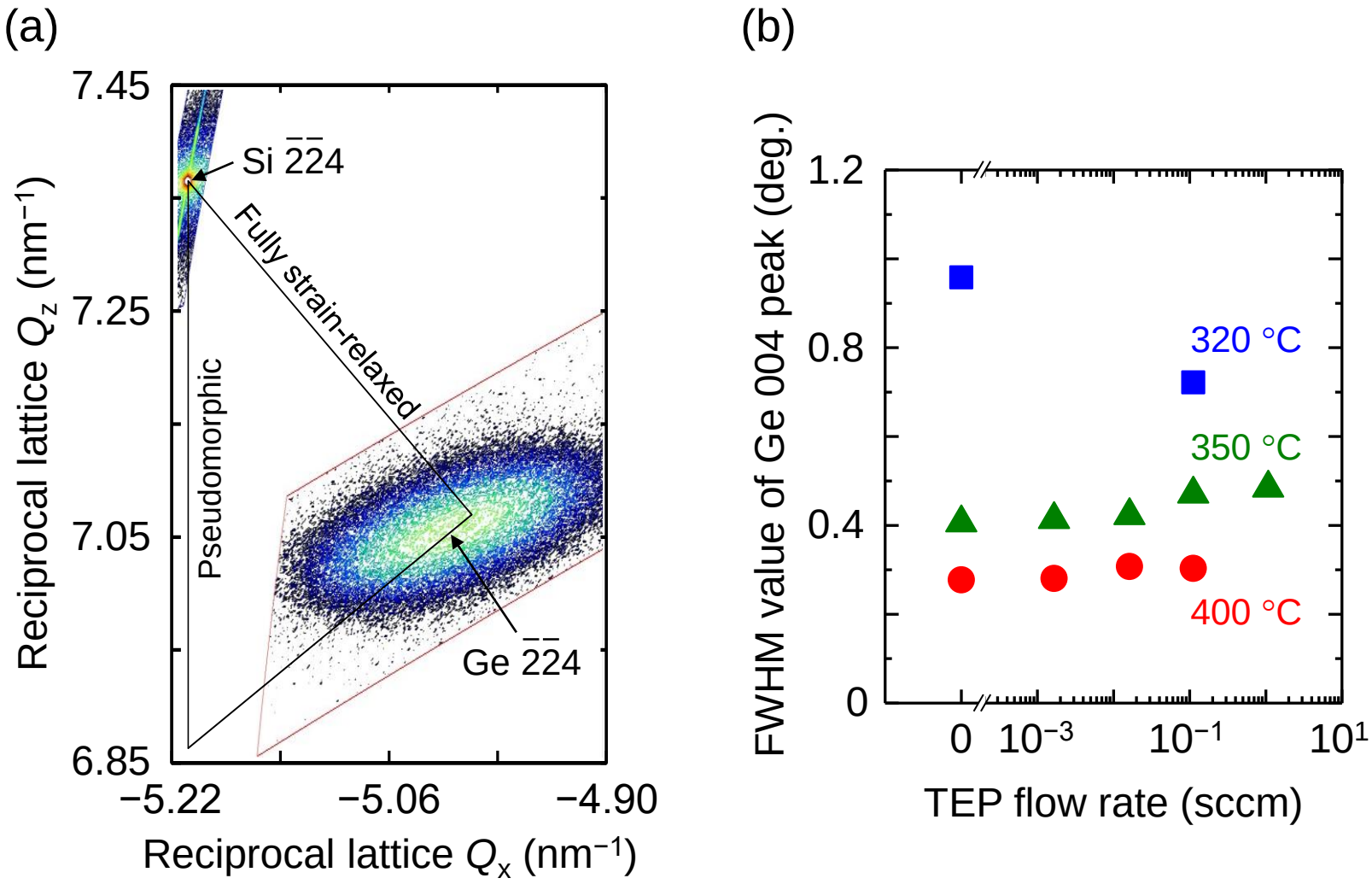
(a)
7.45
7.25
7.05
6.85
Reciprocal lattice Q_z (nm^{-1})
Si $\bar{2}\bar{2}4$
Fully strain-relaxed
Pseudomorphic
Ge $\bar{2}\bar{2}4$
−5.22
−5.06
−4.90
Reciprocal lattice Q_x (nm^{-1})
(b)
FWHM value of Ge 004 peak (deg.)
1.2
0.8
0.4
0
320 °C
350 °C
400 °C
0
10^{-3}
10^{-1}
10^{1}
TEP flow rate (sccm)

Fig. 5

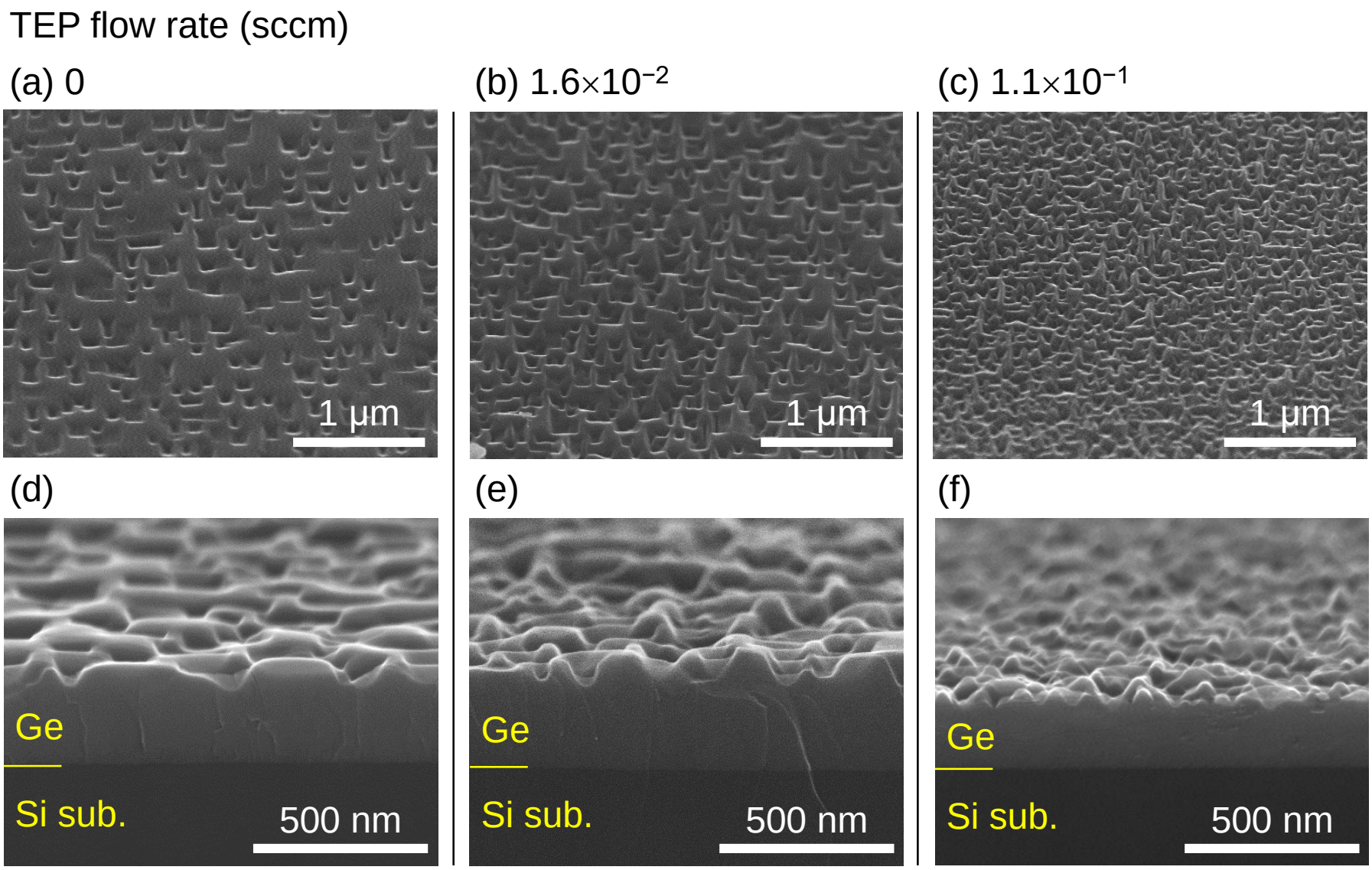
TEP flow rate (sccm)
(a) 0
(b) 1.6×10⁻²
(c) 1.1×10⁻¹
1 μm
1 μm
1 μm
(d)
(e)
(f)
Ge
Si sub.
500 nm
Ge
Si sub.
500 nm
Ge
Si sub.
500 nm

Fig. 6

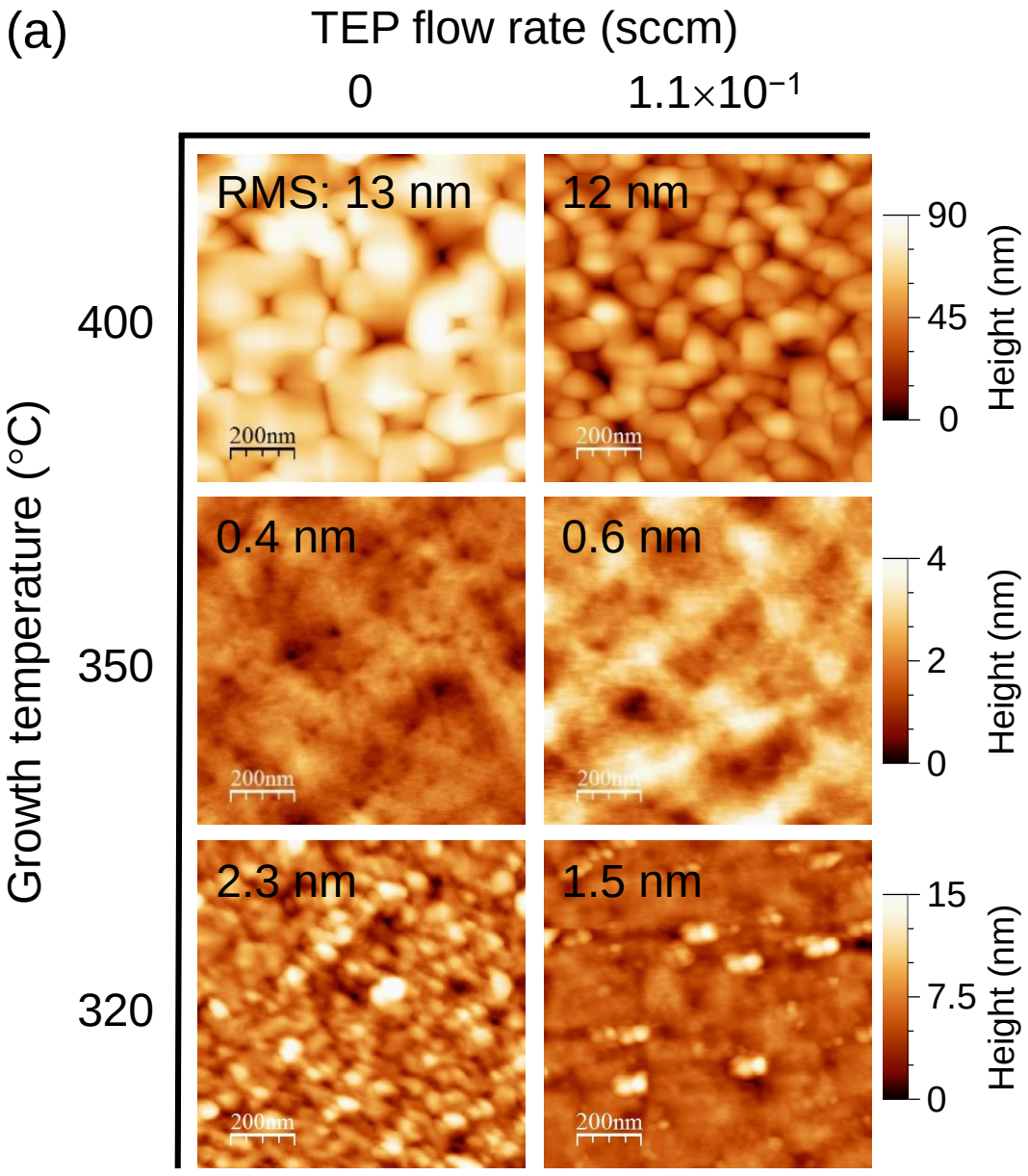
(a)
TEP flow rate (sccm)
0
1.1×10⁻¹
Growth temperature (°C)
400
350
320
RMS: 13 nm
12 nm
0.4 nm
0.6 nm
2.3 nm
1.5 nm
200nm
90
45
0
4
2
0
15
7.5
0
Height (nm)

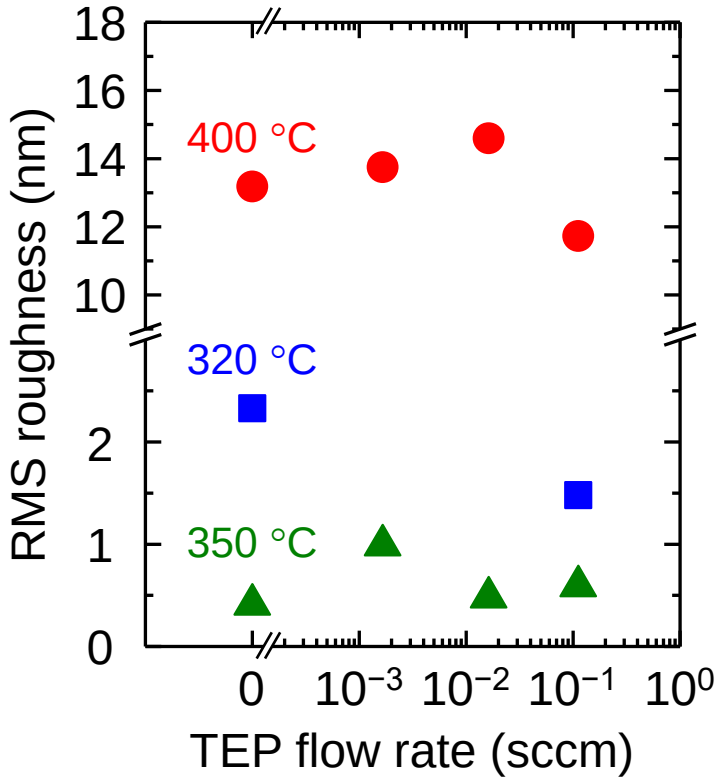
(b)
RMS roughness (nm)
18
16
14
12
10
2
1
0
400 °C
320 °C
350 °C
0
10⁻³
10⁻²
10⁻¹
10⁰
TEP flow rate (sccm)

Fig. 7

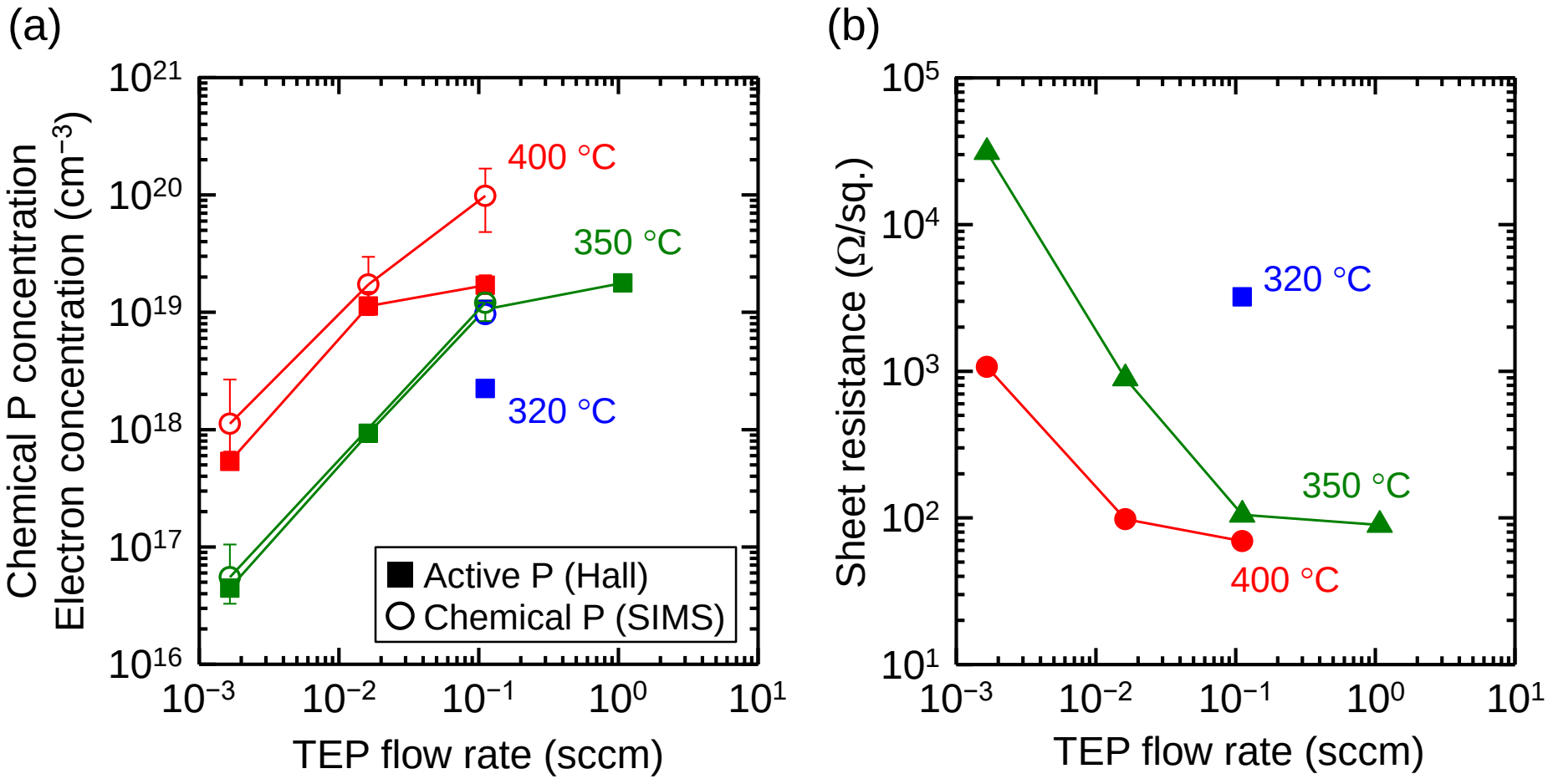
(a)
Chemical P concentration
Electron concentration (cm⁻³)
10²¹
10²⁰
10¹⁹
10¹⁸
10¹⁷
10¹⁶
400 °C
350 °C
320 °C
Active P (Hall)
Chemical P (SIMS)
10⁻³
10⁻²
10⁻¹
10⁰
10¹
TEP flow rate (sccm)
(b)
Sheet resistance (Ω/sq.)
10⁵
10⁴
10³
10²
10¹
320 °C
350 °C
400 °C
10⁻³
10⁻²
10⁻¹
10⁰
10¹
TEP flow rate (sccm)

Fig. 8

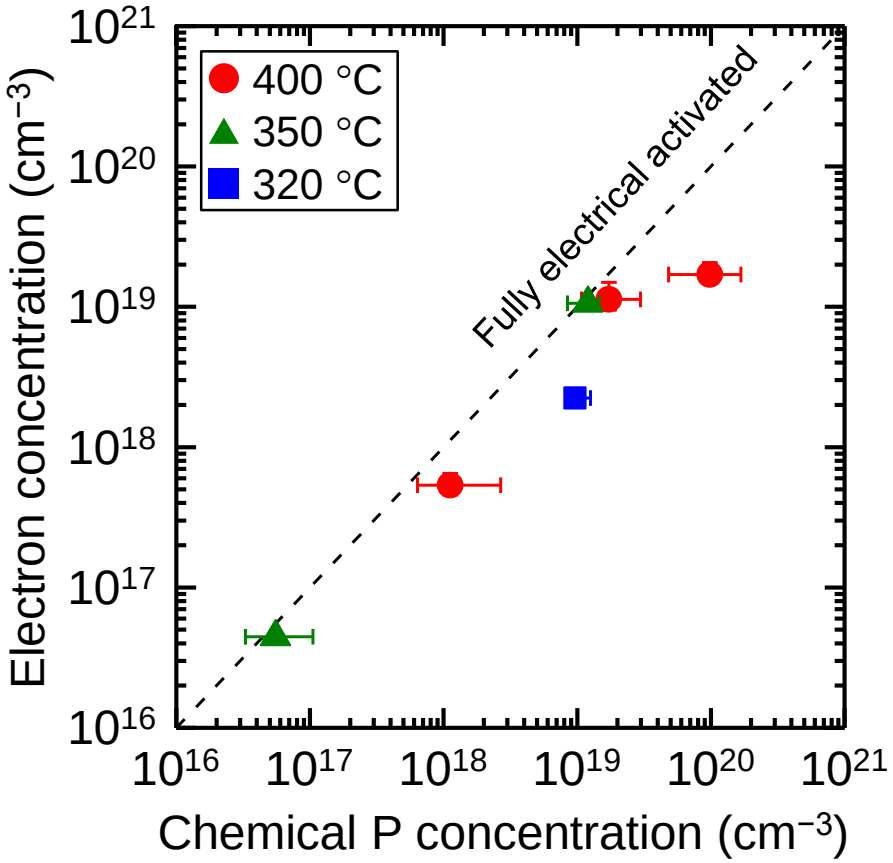
400 °C
350 °C
320 °C
Fully electrical activated
Electron concentration (cm⁻³)
Chemical P concentration (cm⁻³)
10¹⁶
10¹⁷
10¹⁸
10¹⁹
10²⁰
10²¹

Fig. 9

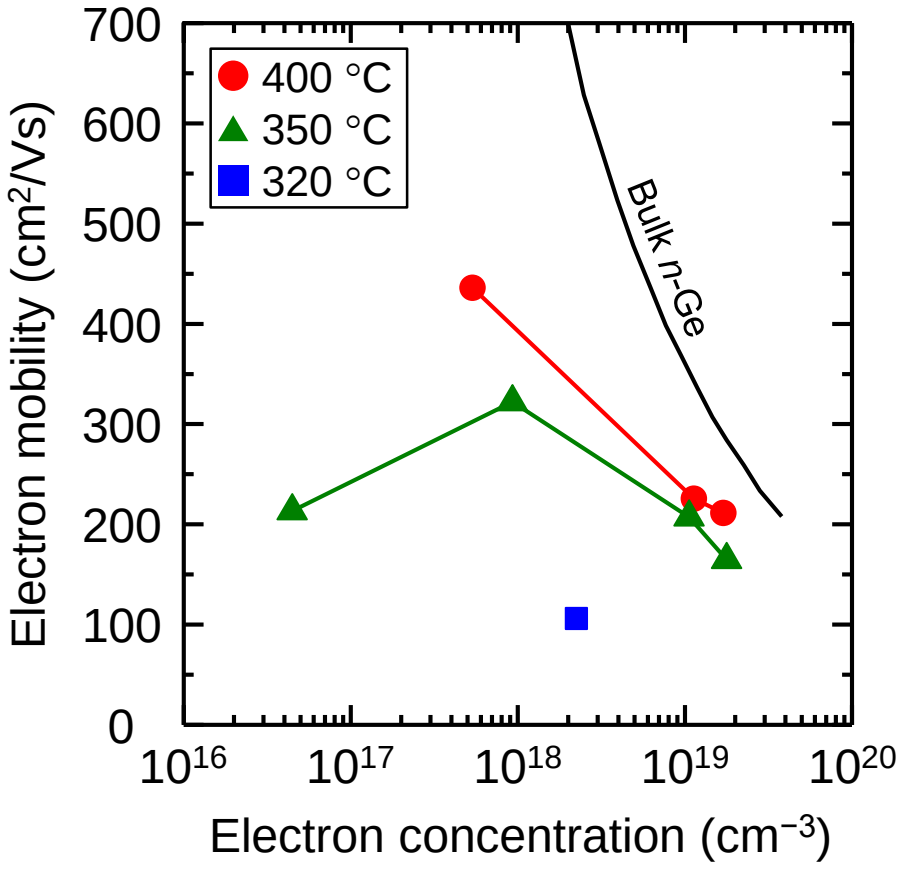
400 °C
350 °C
320 °C
Bulk n-Ge
Electron mobility (cm²/Vs)
Electron concentration (cm⁻³)
0
100
200
300
400
500
600
700
10¹⁶
10¹⁷
10¹⁸
10¹⁹
10²⁰